The modelling of fluidized bed dryer for spherical and non spherical particles

Abanti Sahoo*, Biswajit Swain**, and Soumya Sanjeeb Mohapatra*,†

*Department of Chemical Engineering, National Institute of Technology, Rourkela, India
**Department of Metallurgical and Materials Engineering, National Institute of Technology, Rourkela, India

Abstract−We designed and modelled a fluidized bed dryer. Based on the literature, modelling of a bed dryer is carried out for two situations: for spherical and non-spherical particles. Two case studies were taken from the literature for modelling the fluidized bed dryer for naphthalene balls and mushroom slices. Fluidized bed dryer design was carried out with respect to diffusivity of the bed materials. Drying characteristics in terms of effective diffusivity were studied for naphthalene balls and mushroom slices using a tapered fluidized bed dryer. The variation of effective diffusivity was obtained with change in inlet air temperature, velocity, thickness of slab and drying time. Experimental effective diffusivity as obtained from literature was compared with model predicted values, provided lower deviations with RMSE of less than 8.28% for spherical naphthalene balls and 0.936% for the mushroom slices. Mass transfer coefficient obtained for naphthalene balls was in the range of 2.1×10^{-4} to 4.857×10^{-3} m sec^{-1}. The diffusivity constant was evaluated using Fick's diffusion equation assuming surface moisture in equilibrium with the surrounding atmosphere. The value of diffusivity constant (D_0) obtained is 1.828×10^{-9} m^{2}sec^{-1} and the value of activation energy (E_a) obtained is 4.523 kJ mol^{-1}.

Keywords: Activation Energy, Fick's Diffusion Model, Fluidized Bed Dryer, Variable Effective Diffusivity, Naphthalene Balls, Mass Transfer Coefficient

INTRODUCTION

A model is a demonstration of physical phenomena of a system while express in terms of mathematical or analytical way which are capable to specify, correlate, validate and predict the behaviour or structure of a system or the phenomena with a feasible solution of model determination. Mathematical modeling of the process and the experimental setup are the most significant aspects of drying technology [1]. The modelling is fundamentally based on the design of a set of equations which aims to illustrate or define the system as accurately as possible. These mathematical models of the drying processes are used for designing new or improving existing drying systems.

Drying is one of the very essential unit operations in heat and mass transfer operations that converts the feed material of solid or semi-solid into a solid product of relatively lower moisture content [2,3]. This complex phenomenon involves the application of thermal energy supplied to the material by the means of drying air, which results in the transfer of thermal energy by the surrounding to the material surface by convection mechanism and, then, from the surface to the inside of the material by conduction. This thermal energy results in the transfer of moisture within the material to its surface by diffusion and then water removal from the surface to the surrounding by evaporation. Drying finds application in almost all industrial sectors, such as agriculture, manufacturing of pulp and paper, polymer [4], ceramic, chemical, textile and pharmaceutical. Drying is the most frequently used food preserving

technique and thereby enhances shelf life and improves product quality [5]. Drying leads to a reduction in bulk, weight and volume of the dried products leading to reducing handling, packaging, transportation and storage requirement and cost [6].

Fluidized bed dryers work on the principle of fluidization where a bed of loosely packed solid particles acquires some of the properties of a fluid when a gas is blown vertically upward through it. Due to increase in gas velocity, a condition occurs when the bed is said to be fluidized when the drag force equals the weight of the particles. The transition from a fixed to a bubble-free fluidized bed is denoted by the minimum fluidization velocity [7]. Fluidized beds are extensively used in industrial sectors for drying of the particulate and granular solids, such as grains, cereals, fertilizers, chemicals, pharmaceuticals, minerals and plastics. The main advantage of fluidized bed drying over other drying techniques is the interaction of large contact surface area between solids and fluidizing air that results in high heat and mass transfer rates, resulting in uniform product quality due to complete mixing and high drying capacity. Hence, rapid heat and moisture transfer takes place between solid and fluidizing air, which shortens drying time and prevents damage to heat sensitive materials.

LITERATURE REVIEW

Fluidized bed dryers are unique in design and generally product specific, so various mathematical models are predicted to describe the drying characteristics [8]; thus drying performance can be predicting by using suitable thin-layer models. During these operations, a layer of the material is fully bare to drying conditions at the temperature of hot air, thus enhancing the drying process. Due to thin layer characteristics, lumped parameter models are suitable for

thin-layer drying. The most important aspects of thin-layer drying technology are the mathematical modelling of the drying process in estimating the drying kinetics, which describes the most suitable operating conditions, drying behavior and improving the drying process from the experimental data [6]. These models are classified into three groups--theoretical, semi-theoretical and empirical models--that are very useful for predicting drying nature and also for design purposes, but these are valid only within the applied drying conditions.

Theoretical models are generally the solution of Fick's second law of diffusion, which considers both the internal and external resistances to moisture transfer. It involves the geometry, mass diffusivity and conductivity of the material. The semi-theoretical models are derived from a theoretical model or from its simplified form by introducing a new model or empirical constants. Empirical models are completely derived from experimental data and do not have any physical interpretation, as they do not follow the fundamental laws of drying to show the relationship between the rate constant and moisture content. The relation between the average moisture content and drying time can be developed by these models.

During the actual operation, no particular model can be implemented to describe the drying kinetics due to the effect of various operating parameters (drying condition, product characteristics and technique of drying). Therefore, the drying kinetics models are very much important [9]. Among various parameters, the drying temperature and material thickness are the most important parameters of drying vegetables [10]. The drying kinetics was obtained by varying inlet air temperature, and the Thompson model out of 15 different thin layer models was found to be satisfactory [11]. The effective moisture diffusivity of dried culinary banana slices [12], and paddy [13] increased with increased in drying temperature, and consequently the drying time decreased. It was observed that the inlet air velocity was significant as compared to inlet air temperature on the quantity of oil of dried coconut [14]. The drying rate was found to increase significantly with increase in temperature and flow rate of the heating medium, while decrease with increase in solids holdup as for millets [15], oil palm frond [16], and potato slices [17]. On increasing the particle size, the drying process slows as the evaporation from the surface reduces, indicating high internal mass transfer resistance due to much longer diffusional paths within the solids. The shape factor is integrated into the kinetics models of drying to reduce the effect of product shape on the drying process [18]. It has been shown that if ratio of particle volume and its external surface area is taken as characteristic dimension of an irregular shaped particle, the solution of a simultaneous diffusion equation is largely independent of the particle shape [19].

Naphthalene is a special compound in terms of its properties and chemical structure. It is a flammable white solid with the formula $C_{10}H_8$ and the structure of two fused benzene rings. Due to its bicyclic aromatic structure, it is also a polycyclic aromatic hydrocarbon, making it a more volatile compound [20]. However, naphthalene sublimes rapidly at room temperature. Here, the fluidized bed dryer is used to provide necessary conditions for the measurement of the variation in diffusivity of naphthalene by varying certain parameters.

PROPOSED METHODOLOGY

1. For spherical Geometry-naphthalene Balls

Fick's first law gives the relation between diffusive flux to the concentration, where the flux goes from region of high concentration to region of low concentration, which is due to the nearby relative concentration gradient in the system. Therefore, Fick's first law can be defined as

$$J_{AZ} = -\frac{D_{AB}}{RT}\left(\frac{dP_A}{dz}\right) \tag{1}$$

where, D_{AB} is the diffusivity (m^2sec^{-1}), J_{AZ} is diffusional flux (mole $m^{-2}sec^{-1}$), R is the universal gas constant (8.3145 J mol^{-1} K^{-1}), T is the absolute temperature (K), P_A is the partial pressure of A (in Pa), and z is position (m). Here, the negative sign indicates that the diffusion occurs in the direction of drop in concentration. Since diffusion occurs in radial direction, the total flux associated with particles includes both molecular (self-diffusive) and convective flux, which can be given as

$$N_A = -\frac{D_{AB}}{RT}\left(\frac{dP_A}{dr}\right) + \frac{P_A}{P}(N_A + N_B) \tag{2}$$

For non-diffusing stagnant medium B, putting $N_B = 0$ and rearranging, we get

$$N_A = -\frac{D_{AB}P}{RT(P-P_A)}\left(\frac{dP_A}{dr}\right) \tag{3}$$

Considering, a thin spherical shell of radius r and thickness Δr at any instant time of t in which dispersion occurs around the solid as shown in Fig. 1. This is a binary system involving diffusion of molecule A into the surrounding non-diffusing medium B. Then,

Rate of input of A into the thin shell (at r=r): $(4\pi r^2)N_{A|r}$
Rate of output of A from the thin shell (at r=r+Δr): $(4\pi r^2)N_{A|r+\Delta r}$

Here, we assume that the substance size changes so steadily that the diffusion of the substance through the surrounding air happens essentially at steady state. By applying steady state mass balance,
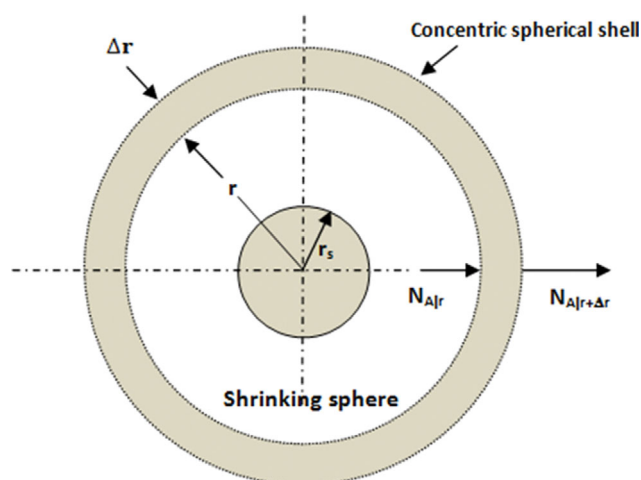

Fig. 1. A schematic demonstrating shell equalisation for mass exchange from a sphere.

Input–output=accumulation

$(4\pi r^2)N_{A|r} - (4\pi r^2)N_{A|r+\Delta r} = 0$

Dividing both sides by Δr and taking limit $\Delta r \to 0$

$$\lim_{\Delta r \to 0} \frac{(4\pi r^2)N_{A|r} - (4\pi r^2)N_{A|r+\Delta r}}{\Delta r}$$

$$\Rightarrow \frac{d(4\pi r^2 N_A)}{dr} = 0$$

$$\Rightarrow 4\pi r^2 N_A = \text{constant} = W \qquad (4)$$

Here, W is the rate of sublimation, Eq. (4) shows a very important result for steady state diffusion through a variable area and can be generalized as product of area and flux to be constant which is equal to the rate of flow of quantity.

On combining Eq. (3) and (4), by comparing N_A, we get

$$\frac{dP_A}{P - P_A} = -\frac{WRT}{4\pi D_{AB}P}\frac{dr}{r^2} \qquad (5)$$

The rate of sublimation (W) from surface to infinity can be obtained by integrating Eq. (5) using conditions,

$P_A = P_{As}$ at $r=r_s$ (at surface)

$P_A = P_{A\infty}$ at $r=\infty$ (At surface)

where, P_{As} and $P_{A\infty}$ are the vapor pressure of the molecule at the surface and infinity respectively. Hence, by integrating, we get

$$W = -\frac{4\pi D_{AB}Pr_s}{RT}\ln\frac{P - P_{A\infty}}{P - P_{As}} \qquad (6)$$

Here we considered that the material variations of the solid substrate arise during drying that cause variation of the diffusivity that makes it reasonable to consider these variations as a function of time. Hence, the proposed empirical expression for D_{AB} is given as

$$D_{AB} = D_i(1 + F_0) \qquad (7)$$

where, D_i is the initial effective diffusivity, and F_0 is the Fourier number ($F_0 = D_i t/r^2$) used for the non- dimensionless time.

Hence Eq. (6) can be written as

$$W = -\frac{4\pi D_i(1 + F_0)Pr_s}{RT}\ln\frac{P - P_{A\infty}}{P - P_{As}} \qquad (8)$$

In the macroscopic view, rate of sublimation can be given as the rate of change of mass as

$$W = -\frac{d}{dt}\left(\frac{4}{3}\pi r_s^3 \frac{\rho_A}{M_A}\right) = -4\pi \frac{\rho_A}{M_A}r_s^2\frac{dr_s}{dt} \qquad (9)$$

Here, the negative sign indicates that the size of the solid decreases with time.

On equating Eq. (8) and (9), by eliminating W, we get

$$-4\pi \frac{\rho_A}{M_A}r_s^2\frac{dr_s}{dt} = -\frac{4\pi D_i(1 + F_0)Pr_s}{RT}\ln\frac{P - P_{A\infty}}{P - P_{As}}$$

At time t=0, the molecule diameter is d_p and at time t it is $d_{p'}$. The change in the molecule size over considerable period of time can be obtained by integrating the above equation as

$$d_p^2 - d_{p'}^2 = \frac{16PM_A d_p^2((1 + F_0)^2 - 1)}{RT\rho_A}\ln\frac{P - P_{A\infty}}{P - P_{As}} \qquad (10)$$

Here, initial effective diffusivity can be obtained from Eq. (9).

2. For Non-spherical Geometry-Mushroom Slices

The average moisture content can be expressed in a non-dimensional moisture ratio as

$$M_R = \frac{M_t - M_e}{M_i - M_e} \qquad (11)$$

where M_R is the dimensionless moisture ratio, M_t is the moisture content at time t, M_i and M_e are the initial and equilibrium moisture contents on dry basis, respectively.

The moisture loss during falling rate period is an internally controlled process. Internal mass transfer may occur by several mechanisms, such as molecular diffusion (liquid and vapor), capillary flow, Knudsen diffusion, surface diffusion or combinations of these. Usually, all these mechanisms are lumped together into an effective transport coefficient to describe the mass flux. Fick's second law equation for one-dimensional diffusion for plate (or slab) geometry is given as

$$\frac{\partial M}{\partial t} = D_{eff}\frac{\partial^2 M}{\partial h^2} \qquad (12)$$

where, M is the average moisture content, D_{eff} is the effective moisture diffusivity (in $m^2 sec^{-1}$), t is the drying time (in sec) and h is the half-slab (or slice) thickness (in m)

The initial and boundary conditions are

$M(h, 0) = M_i$ at t=o

$M(h_0, t) = M_e$ at $h=h_0$ (at the surface)

$M(0, t) = $ finite at h=0 (at the centre)

We considered that the material variations of the solid substrate arise during drying that causes variation of the diffusivity, which makes it reasonable to consider these variations as a function of time. Hence, the proposed empirical expression for D_{eff} is given as

$$D_{eff} = D_i(1 + F_0) \qquad (13)$$

where, D_i is the initial effective diffusivity, and F_0 is the Fourier number ($F_0 = D_i t/h^2$) used for the non- dimensionless time.

Based on assumptions on boundary conditions for thin layer drying, such as product sizes are homogeneous and isotropic, mass transfer is symmetrical with uniform initial moisture distribution, negligible external resistance, negligible pressure and temperature gradients, product's surface moisture undergoes moisture equilibrium, and negligible shrinkage during drying. The analytical solution of the diffusion equation for above initial and boundary conditions is given as

$$M_R = \frac{8}{\pi^2}\sum_{n=0}^{\infty}\frac{1}{(2n+1)^2}\exp\left(-\frac{(2n+1)^2\pi^2((1+F_0)^2-1)}{8}\right) \qquad (14)$$

On considering a longer drying period, only the first term of the series dominates and the initial uniform moisture content to be unity by neglecting the term $(8/\pi^2)$. The above equation can be expressed as

Table 1. Experimental and predicted data for diffusivity of naphthalene balls

Time (min)	Temperature (°C)	Velocity (m sec⁻¹)	Initial weight (gm)	Final diameter (cm)	D (lit) (m²sec⁻¹)	D (cal) (m²sec⁻¹)	% Deviation
25	60	3.8	200	1.74	2.69E-09	2.63E-09	2.228
25	70	3.8	150	1.55	8.2E-09	7.72E-09	6.277
25	80	3.8	123	1.4	2.11E-08	1.82E-08	13.645
25	90	3.8	91	1.33	4.92E-08	3.72E-08	24.394
10	70	3.8	200	1.8	6.41E-09	6.27E-09	2.13
15	70	3.8	165	1.76	6.96E-09	6.72E-09	3.381
20	70	3.8	151	1.71	7.55E-09	7.19E-09	4.752
25	70	3.8	140	1.65	8.07E-09	7.57E-09	6.162
25	70	0.975	200	1.78	2.31E-09	2.27E-09	1.927
25	70	1.95	140	1.73	4.34E-09	4.19E-09	3.504
25	70	2.875	126	1.65	6.29E-09	5.98E-09	4.93
25	70	3.8	116	1.5	1.12E-08	1.03E-08	8.217
25	70	308	200	1.51	1.10E-08	1.01E-08	8.043
25	70	3.8	250	1.64	4.51E-09	4.35E-09	3.632
25	70	3.8	300	1.73	2.86E-09	2.79E-09	2.364
25	70	3.8	350	1.79	1.99E-09	1.96E-09	1.669

$$M_R = \exp\left(-\frac{\pi^2((1+F_0)^2-1)}{8}\right) \qquad (15)$$

The value of initial moisture diffusivity (D_i) can be determined from above equation. The relationship between effective diffusivity and temperature is assumed to be an Arrhenius function of the type

$$D_{eff} = D_0 \exp\left(-\frac{Ea}{RT}\right) \qquad (16)$$

where, D_0 is the diffusivity constant at infinite drying temperature ($m^2 s^{-1}$), R is the universal gas constant ($8.3145\,J\,mol^{-1}\,K^{-1}$), Ea is the activation energy ($kJ\,mol^{-1}$), which is the minimum energy required to break water-solid or water-water interactions and to move the water molecules from one point to another in the solid, and T is the absolute temperature (K). The value of D_0 and Ea can be obtained on plotting $\ln(D_{eff})$ with ($1/T$) on changing the above equation in logarithmic form to a new linear equation as

$$\ln(D_{eff}) = \ln(D_0) - \frac{Ea}{RT} \qquad (17)$$

RESULTS AND DISCUSSION

1. For Spherical Geometry-naphthalene Balls

In the present study, diffusivity of naphthalene balls (in the form of a sphere) through a fluidized bed dryer were determined using Fick's diffusion equation. Table 1 shows the comparison of the experimental and predicted diffusivity values for the variation in temperature, air velocity, drying time and thickness of the material for which the minimum and maximum deviation is 1.669 and 24.394%, respectively. The RMSE for the whole data comes out to be 8.28%, which shows good agreement between the experimental and predicted values for the diffusivity.

The variation of diffusivity obtained from experimental and predicted model data at different temperature starting with initial weight

of bed as 200 gm and at constant velocity of 3.8 m sec⁻¹ is shown in Fig. 2. By increasing the air temperature, it was observed that the diffusivity increased rapidly with increase in temperature. This is because on increasing temperature, mass and heat transfer rate
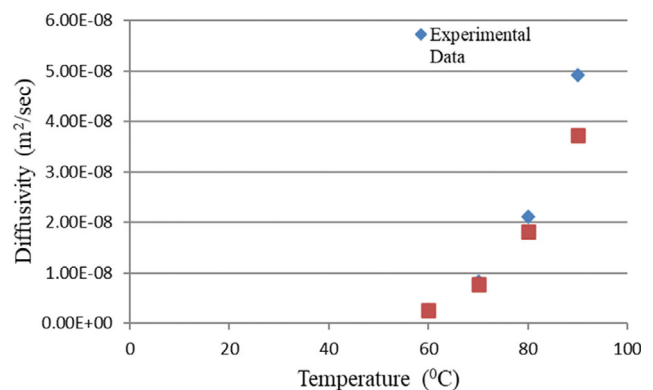
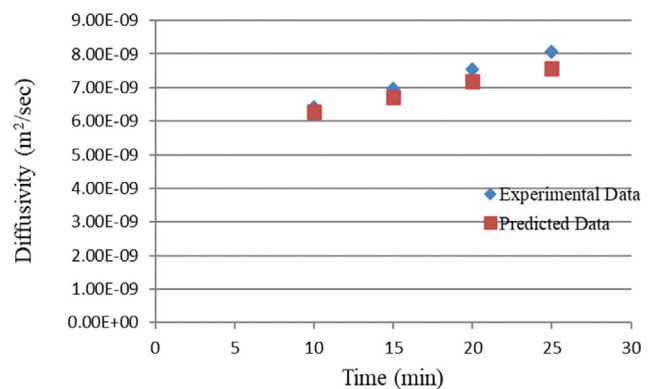**Fig. 2. Variation of diffusivity with temperature for naphthalene balls.**

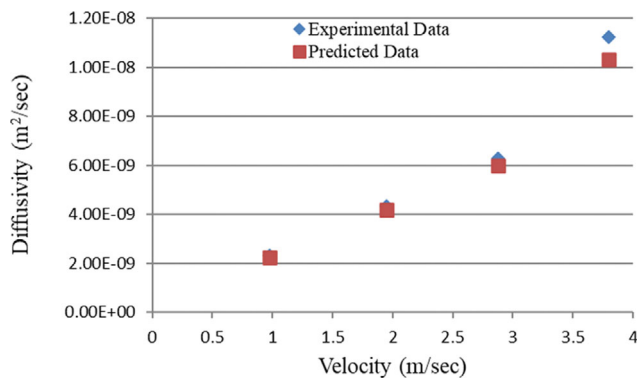**Fig. 3. Variation of diffusivity with time for naphthalene balls.**

Fig. 4. Variation of diffusivity with velocity for naphthalene balls.

Fig. 5. Variation of diffusivity with initial weight of bed for naphthalene balls.

are increased, which increases the driving forces, and it is also concluded that there is significant reduction in size of the naphthalene balls.

Fig. 3 shows the variation of diffusivity obtained from experimental and predicted model data at different sublime time starting with initial weight of bed as 200 gm and at velocity of 3.8 m sec^{-1}. It was observed that the diffusivity increased linearly with time since the regular heating of the material results increase in diffusion.

Fig. 4 shows the variation of diffusivity obtained from literature and proposed equation at different velocity starting with initial weight of bed as 200 gm and at constant temperature of 70 °C. It was observed that the diffusivity increases with velocity as with increase in air velocity, mass and heat transfer rate are increased, which increases the driving forces.

Fig. 5 shows the variation of diffusivity obtained from experimental and predicted model data at different initial weight of bed at constant temperature of 70 °C and constant velocity of 3.8 msec^{-1}. It was observed that the diffusivity decreased with increase in ini-
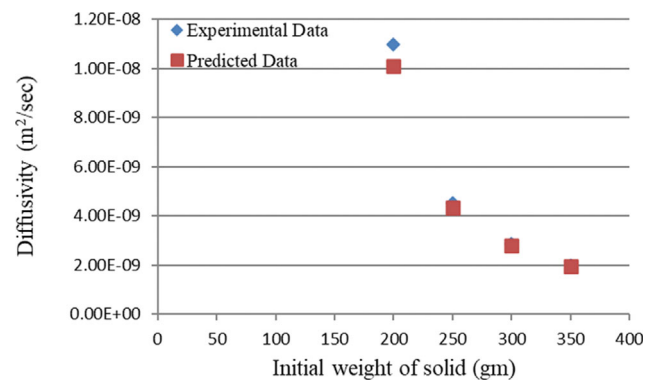
tial weight of bed. This is because buoyant force provided by fluidizing air is the same but weight of the material increases, which results in decrease in agitation and turbulency of the particle.

Mass transfer coefficient is a diffusion rate constant that relates the mass transfer rate; hence, mass transfer kinetics was developed using mass transfer coefficient and in turn diffusivity data with the temperature (Table 2). The Sherwood number, which is called as the mass transfer Nusselt number, represents the ratio of convective to diffusive mass transport and is defined as follows:

$$Sh = \frac{kL}{D} = \frac{\text{Convective mass transfer rate}}{\text{Diffusive mass transfer rate}}$$

where, L is the characteristic length (m) for sphere it is the radius, D is the mass diffusivity (m^{2}sec^{-1}) and k is the mass transfer coefficient (in m sec^{-1}). Mathematical expression of Sherwood number for the spherical particle is given by
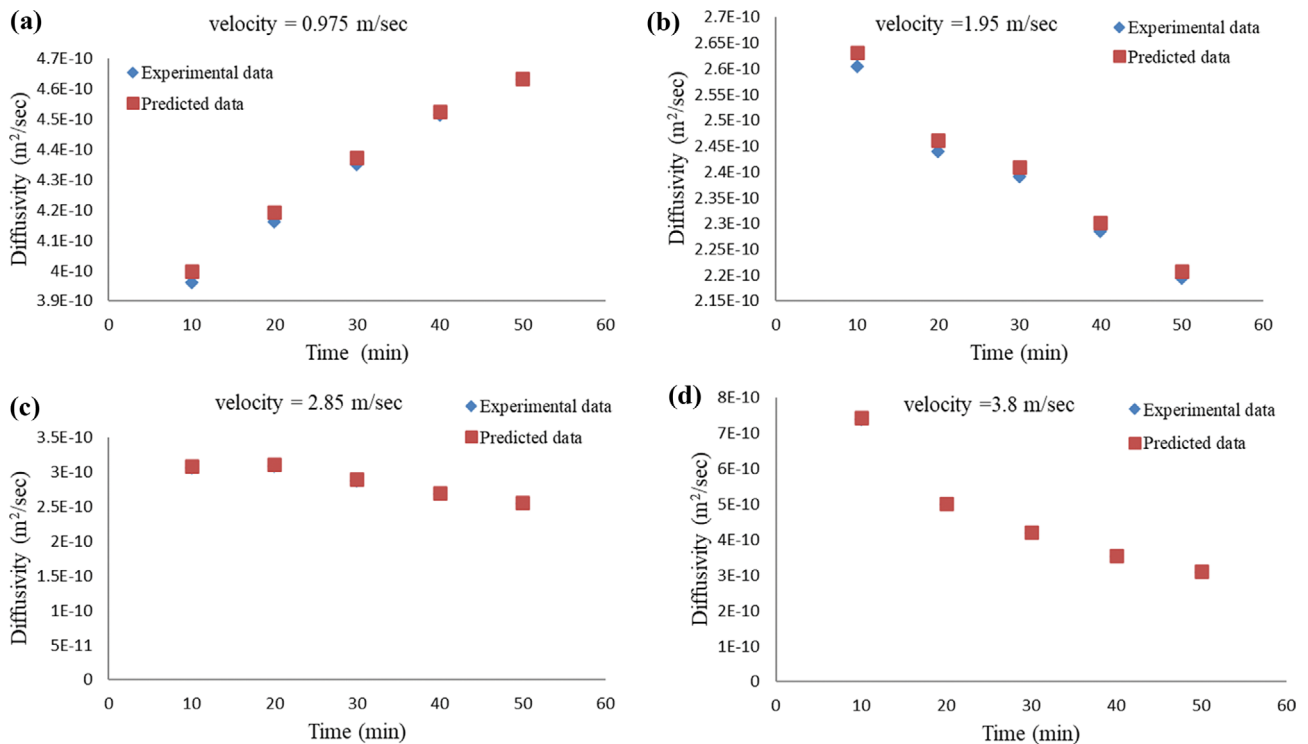
$$Sh = 2 + 0.6 \, (Re)^{1/2} (Sc)^{1/3} \tag{18}$$

Table 2. Mass transfer coefficient for naphthalene balls

Variation parameter		Sherwood number	Mass transfer coefficient
Temperature (°C)	60	1,595.022	0.000461
	70	1,058.718	0.001003
	80	727.7256	0.002007
	90	690.8052	0.004857
Time (min)	10	1,188.953	0.000819
	15	1,138.359	0.00088
	20	1,089.658	0.000935
	25	1,056.8	0.000997
Velocity (m sec^{-1})	3.8	930.5675	0.001269
	2.875	1,003.926	0.00073
	1.95	948.0142	0.000462
	0.975	844.0064	0.00021
Initial weight of bed (gm)	200	996.1237	0.001175
	250	1,334.965	0.000647
	300	1,551.159	0.000477
	350	1,748.125	0.000374

Table 3. Experimental and predicted data for diffusivity for mushroom slices

Time (min)	Temperature (^{o}C)	Velocity (m sec^{-1})	Thickness (cm)	Experimental diffusivity $\times 10^{-10}$ (m^{2}sec^{-1})	Predicted diffusivity $\times 10^{-10}$ (m^{2}sec^{-1})	% Deviation
10	50	0.975	1.6	3.9604	3.998	−0.957
20	50	0.975	1.6	4.1620	4.193	−0.75
30	50	0.975	1.6	4.3504	4.373	−0.528
40	50	0.975	1.6	4.5121	4.525	−0.295
50	50	0.975	1.6	4.6297	4.632	−0.06
10	50	1.95	1.6	2.6047	2.631	−1.022
20	50	1.95	1.6	2.4401	2.462	−0.913
30	50	1.95	1.6	2.3902	2.409	−0.805
40	50	1.95	1.6	2.2844	2.301	−0.712
50	50	1.95	1.6	2.1945	2.208	−0.625
10	50	2.875	1.6	3.0558	3.086	−1
20	50	2.875	1.6	3.0788	3.105	−0.853
30	50	2.875	1.6	2.8702	2.891	−0.737
40	50	2.875	1.6	2.6814	2.698	−0.637
50	50	2.875	1.6	2.541	2.555	−0.544
10	50	3.8	1.6	7.3883	7.447	−0.794
20	50	3.8	1.6	4.9848	5.018	−0.672
30	50	3.8	1.6	4.1893	4.212	−0.55
40	50	3.8	1.6	3.5354	3.552	−0.477
50	50	3.8	1.6	3.0951	3.108	−0.415
50	40	3.8	1.6	2.3485	2.362	−0.589
50	60	3.8	1.6	5.6136	5.604	0.1652
50	70	3.8	1.6	11.825	11.64	1.5406
50	50	3.8	1.2	2.8778	2.844	1.1711
50	50	3.8	0.8	1.833	1.803	1.6618
50	50	3.8	0.625	1.6585	1.618	2.4254

Fig. 6. Variation of effective diffusivity with drying time at different velocities.
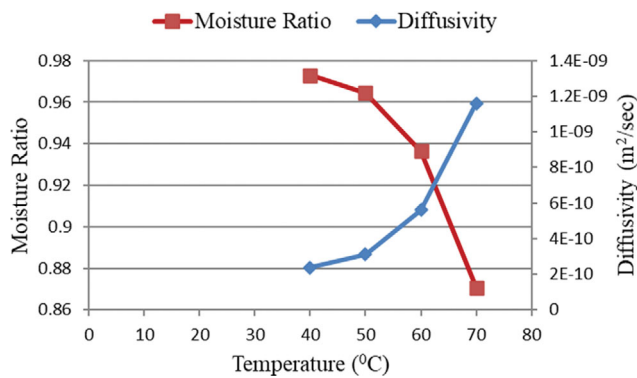
Fig. 7. Variation of effective diffusivity and moisture ratio with temperature for mushroom slices.
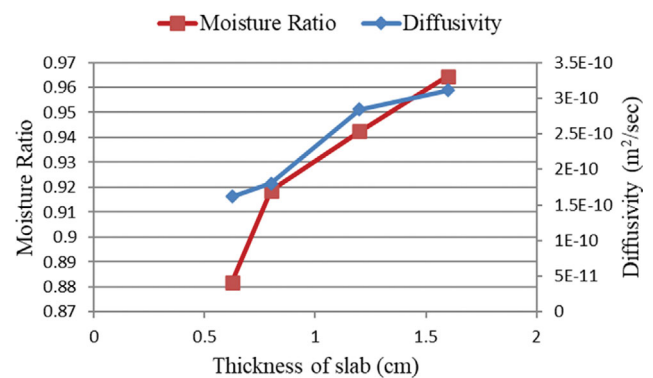

Fig. 8. Variation of effective diffusivity and moisture ratio with thickness of mushroom slice.

2. For Non-spherical Geometry-Mushroom Slices

In the present study, diffusivity of mushroom dried (in the form of slab) through a fluidized bed dryer was determined using Fick's diffusion equation. Table 3 shows the comparison of the experimental and predicted diffusivity values for the variation in temperature, fluidizing velocity, drying time and thickness of the material for which the minimum and maximum deviation are 0.06 and 2.4254%, respectively. The RMSE for the whole data comes out to be 0.936%, which shows good agreement between the experimental and predicted values for the diffusivity.

Fig. 6 shows the variation of experimental and predicted diffusivity with drying time at four different velocities. In Fig. 6(a) the effective diffusivity increases slightly with drying time at low velocity. Fig. 6(b) and (c) show the slight decrease in the diffusivity with drying time with moderate velocity, whereas Fig. 6(d) shows a large decrease in diffusivity with drying time at high velocity. It can be concluded that the predicted model has a good agreement in showing the nature of the experimental data.

From Fig. 6, it was observed that velocity shows a dual nature for diffusivity. With the same temperature of 50 $^{\circ}$C, at low velocity the diffusivity increases, whereas at high velocity diffusivity decreases. It is because at low velocity there is greater internal resistance, whereas at high velocity, although the heat transfer rate is high, the external resistance becomes very high as compared to internal resistance and, thus, becomes rate limiting.

The values for the plot were obtained at velocity of 3.8 m sec^{-1} and for drying time of 50 minutes. By increasing the air temperature, the mass and heat transfer rate are increased due to the increase in the driving forces. Similar behavior can be obtained from Fig. 7; as with increase in temperature, there is a sharp increase in effective diffusivity and also a sharp decrease in moisture ratio signifying a large amount of moisture transfer at high temperature.

The values for the plot were obtained at velocity of 3.8 m sec^{-1} and drying time of 50 minutes, which shows that the drying process is externally controlled. With increase in thickness of the slab, the reduction in moisture ratio decreases, which is due to the higher heat and mass transfer resistance offered by the thicker material, as can be seen through Fig. 8. On the other hand, from Fig. 6(d), for velocity 3.8 m sec^{-1}, effective diffusivity decreases, but here the increase in thickness further strengthens the internal resistance, as
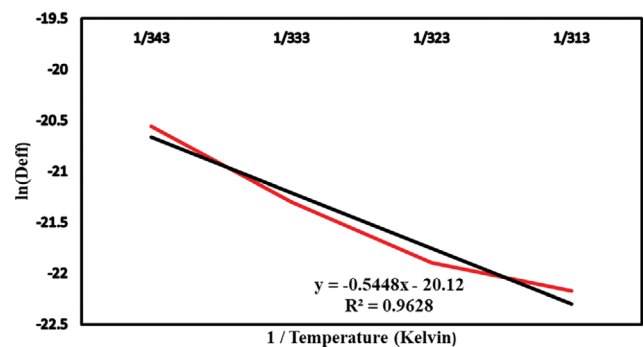

Fig. 9. Variation of ln(D$_{eff}$) versus 1/temperature for mushroom slices.

much thicker material requires much longer drying length. Hence, the effective diffusivity increases as both the internal and external resistances are comparable.

Fig. 9 shows the relation of effective diffusivity (lnD$_{eff}$) and absolute temperature to be linear, which relates to Arrhenius relation between effective diffusivity and temperature. The values for the plot were obtained at velocity of 3.8 m sec^{-1} and for drying time of 50 minutes. The value of R^2 (determination coefficient) is 0.962. From the plot, the value of diffusivity constant (D$_0$) obtained is 1.828×10^{-9} m^{2}sec^{-1} and the value of activation energy (E$_a$) obtained is 4.523 kJ mol^{-1}.

CONCLUSIONS

Drying characteristics in terms of diffusivity were compared for spherical naphthalene balls and non-spherical mushroom slices (in the form of slab). The variation of diffusivity was examined by varying drying parameters, including inlet air temperature, velocity, drying time, initial weight of bed and thickness of the material. The predicted model is based on the variable diffusivity as a function of time in the form of dimensionless Fourier number. It was observed that the predicted model has a good agreement in showing the nature of the experimental data.

For naphthalene balls, a deviation of the model predicted diffusivities from experimental was observed with RMSE of about 8.28%. The diffusivity shows significant increase with temperature that slightly increases with drying time and velocity, whereas decreases

with increase in initial bed weight. Mass transfer coefficients obtained for naphthalene balls were in the range of 2.1×10^{-4} to 4.857×10^{-3} m sec^{-1}.

For mushroom slices, lower deviation of the model predicted effective diffusivity from experimentally determined effective diffusivity was observed with RMSE of about 0.936%. The effective diffusivity was found to increase significantly with increase in drying temperature and slightly with increase in thickness of the material. At lower velocity (for internally controlled process), the effective diffusivity increases slightly with drying time, whereas at higher velocity (for externally controlled process) the effective diffusivity decreases significantly with drying time. The value of diffusivity constant (D_0) obtained is 1.828×10^{-9} m^{2}sec^{-1} and the value of activation energy (E_a) obtained is 4.523 kJmol^{-1}.

REFERENCES

1. S. A. Pérez Cortés, Y. R. Aguilera Carvajal, J. P. Vargas Norambuena, J. A. Norambuena Vásquez, J. A. Jarufe Troncoso, J. P. Hurtado Cruz, A. P. Muñoz Lagos and P. P. Jara Muñoz, *Chem. Eng. Technol.*, **44**, 1567 (2021).
2. M. F. Mohideen, B. Sreenivasan, S. A. Sulaiman and V. R. Raghavan, *Korean J. Chem. Eng.*, **29**, 862 (2012).
3. Y. Choi, S. Maken, S. Lee, E. Chung, J. Park and B. Min, *Korean J. Chem. Eng.*, **24**, 288 (2007).
4. K. Park, H. Kim, S. Maken, Y. Kim, B. Min and J. Park, *Korean J. Chem. Eng.*, **22**, 412 (2005).
5. R. Barathiraja, P. Thirumal, G. Saraswathy and I. Rahamathullah, *J. Mech. Sci. Technol.*, **35**, 2707 (2021).
6. D. I. Onwude, N. Hashim, R. B. Janius, N. M. Nawi and K. Abdan, *Compr. Rev. Food Sci. Food Saf.*, **15**, 599 (2016).
7. D. N. Deomore and R. B. Yarasu, *Processes*, **6**, 195 (2018).
8. N. S. Haron, J. H. Zakaria and M. F. Mohideen Batcha, *IOP Conf. Ser. Mater. Sci. Eng.*, **243**, 012 (2017).
9. S. K. Giri and S. Prasad, *J. Food Eng.*, **78**, 512 (2007).
10. H. Pandey and H. K. Sharma, CBS Publishers & Distributors Pvt Ltd, India (2006).
11. I. L. Pardeshi, S. Arora and P. A. Borker, *Dry. Technol.*, **27**, 288 (2009).
12. P. Khawas, K. K. Dash, A. J. Das and S. C. Deka, *Int. J. Food Eng.*, **11**, 667 (2015).
13. S. Suherman and E. E. Susanto, *IOP Conf. Ser. Mater. Sci. Eng.*, **543**, 012 (2019).
14. C. Niamnuy and S. Devahastin, *J. Food Eng.*, **66**, 267 (2005).
15. C. Srinivasakannan and N. Balasubramanian, *Adv. Powder Technol.*, **20**, 298 (2009).
16. I. Puspasari, M. Z. M. Talib, W. R. W. Daud and S. M. Tasirin, *Dry. Technol.*, **30**, 619 (2012).
17. A. Reyes, P. Moyano and J. Paz, *Dry. Technol.*, **25**, 581 (2007).
18. J. Srikiatden and J. S. Roberts, *Int. J. Food Prop.*, **10**, 739 (2007).
19. R. Aris, *Chem. Eng. Sci.*, **50**, 3897 (1995).
20. P. S. Price and M. A. Jayyock, *Regul. Toxicol. Pharmacol.*, **51**, 15 (2008).